ELSEVIER

Polymer 42 (2001) 3893–3900

polymer

www.elsevier.nl/locate/polymer

Liquid–liquid phase separation in a ternary system of segmented polyetherurethane/dimethylformamide/water: effect of hard segment content

H.K. Lee[a,*], J.Y. Kim[b], Y.D. Kim[b], J.Y. Shin[b], S.C. Kim[b]

[a]*Department of Industrial Chemistry, Chungwoon University, 29, Namjang-Ri, Hongsung-Eub, Hongsung-Gun, Chungnam 350-800, South Korea*
[b]*Center for Advanced Functional Polymers, Korea Advanced Institute of Science and Technology, 373-1, Kusung-Dong, Yusung-Gu, Taejon 305-701, South Korea*

Received 4 February 2000; received in revised form 27 July 2000; accepted 8 August 2000

Abstract

A series of segmented polyurethanes (SPUs) using poly(tetramethylene oxide) (PTMO), 4,4′-methylenebis (phenyl isocyanate) (MDI), and ethylene glycol (EG) with different molar ratios of MDI and PTMO were prepared to study the effects of the hard segment content in SPU on liquid–liquid phase separation in the SPU/dimethylformamide(DMF)/water system. The cloud points were obtained by a titration method and the phase diagrams were calculated based on the Flory–Huggins thermodynamics. The DMF–SPU interaction parameter, χ_{23} was determined by the intrinsic viscosity measurement. The water–SPU interaction parameter, χ_{13} was measured by an equilibrium swelling experiment. As the hard segment fraction in SPU increased, the values of χ_{23} increased slightly and those of χ_{13} decreased significantly. The amount of water to achieve liquid demixing increased systematically with the hard segment content. The χ_{13} values in the practical concentration range were estimated by comparison of the calculated phase diagrams with the experimental cloud points. Liquid–liquid phase separation was coupled with liquid–solid phase separation (crystallization) when the SPU had high concentration of the hard segment. These coupled phenomena in combination with the phase segregation in SPU arising from the incompatibility between the hard and soft segments may be utilized to produce a variety of the morphologies of polyurethane membranes prepared by immersion precipitation. © 2001 Published by Elsevier Science Ltd.

Keywords: Segmented polyurethane; Hard segment content; Polymer solution

1. Introduction

Segmented polyurethanes (SPUs) are multiblock copolymers consisting of hard segment and soft segment of polyether or polyester. These polymers possess many applications as biomaterials due to their excellent physical properties and relatively good biocompatibility [1]. The preparation of biomedical devices such as vascular prostheses often involves formation of porous polyurethane membranes via an immersion precipitation process [2,3]. In this process, a homogeneous polymer solution is contacted with nonsolvent and subsequent exchange of solvent and nonsolvent across the interface results in phase separation into a polymer-rich phase and a polymer-lean phase. Phase separation is continued until the polymer-rich phase is solidified by gelation [4] and/or crystallization of the polymer [4–6].

While the final morphology of the membrane obtained is dictated by the kinetics as well as the thermodynamics of the phase separation, the equilibrium phase diagram is still a good tool for controlling the morphology and interpreting the membrane structure. Knowledge of phase equilibrium enables one to change the conditions for the preparation of membranes such as the temperatures and the compositions of the dope solution and of the coagulation bath to obtain an optimum structure [7].

In the present study, we are concerned with the thermodynamic analysis of a SPU/dimethylformamide (DMF)/water system. In an attempt to investigate the effect of the hard segment content of SPU on liquid–liquid phase separation, we prepared a series of SPUs based on poly(tetramethylene oxide)(PTMO), 4,4′-methylenebis(phenyl isocyanate)(MDI), and ethylene glycol (EG) with different molar ratios of MDI and PTMO. Although a two phase morphology of the bulk SPU due to segmental incompatibility depends on hard segment mobility, system viscosity, and hard segment interaction [8–10], a greater

* Corresponding author. Tel.: +82-41-630-3255; fax: +82-41-634-8740.
E-mail address: hwanklee@cwunet.ac.kr (H.K. Lee).

0032-3861/01/$ - see front matter © 2001 Published by Elsevier Science Ltd.
PII: S0032-3861(00)00707-2

Table 1
Characterization of segmented polyurethanes

Sample code	MDI:PTMO:EG molar ratios	Hard segment weight %[a]	$\overline{M_n}$[b]	$\overline{M_w}$[b]	Density[c] (g/cc)
SPU-1	1:0.600:0.400	18.6	19533	37942	1.0122
SPU-2	1:0.315:0.685	31.7	20222	34749	1.0422
SPU-3	1:0.167:0.833	47.5	27330	56567	1.0809
SPU-4	1:0.091:0.909	62.7	25457	50156	1.1210

[a] Calculated from the amounts of reactants; (MDI + EG)/(PTMO + MDI + EG).
[b] Measured by size exclusion method.
[c] The value at room temperature estimated from additive group contributions [18].

crystallizability of the polymer is expected with increasing hard segment length [11,12]. Liquid demixing during immersion precipitation would be coupled with crystallization [13,14] when the SPU has a high amount of the hard phase volume fraction. We obtained the phase diagram in the ternary system of SPU/DMF/water by a titration method and calculated the binodal curves to investigate the phase separation phenomena involved in polyurethane membrane formation.

2. Liquid–liquid phase equilibrium in ternary solutions

The Flory–Huggins lattice treatment [15,16] is used to describe the thermodynamics of the ternary system for its simplicity. The Flory–Huggins expression is extended with a concentration dependent interaction parameter. The Gibbs free energy of mixing ΔG_M in ternary solutions is given by

$$\Delta G_M/RT = n_1 \ln \phi_1 + n_2 \ln \phi_2 + n_3 \ln \phi_3 + g_{12}(u_2) n_1 \phi_2 + \chi_{13} n_1 \phi_3 + \chi_{23} n_2 \phi_3 \quad (1)$$

where n_i is the number of moles; ϕ_i, the volume fraction of component i; R, the gas constant; and T, the absolute temperature. The subscripts refer to nonsolvent (1), solvent (2), and polymer (3). χ_{13} is the nonsolvent-polymer interaction parameter, and χ_{23}, the solvent-polymer interaction parameter. g_{12} is the nonsolvent-solvent interaction parameter that is assumed to be a function of u_2 with $u_2 = \phi_2/(\phi_1 + \phi_2)$. The effects of the polydispersity of polymer molecules are neglected. Following Flory's recommendation [15], the number-average molecular weight is used for polymers.

The conditions for equilibrium between two liquid phases I and II can be written as

$$\Delta\mu_i^{I} = \Delta\mu_i^{II} \qquad (i = 1, 2, 3) \quad (2)$$

where $\Delta\mu_i$ is the chemical potential of component i. Superscript I and II refer to polymer-rich and polymer-lean phases, respectively. The details about the calculation of binodal curves can be found in the previous publication [17].

3. Experimental

3.1. Preparation of polyurethanes

Segmented polyurethanes were prepared with a one-step solution polymerization method. Predetermined amounts of PTMO (Shinwha Petrochemical, South Korea, M_n, 1990) and EG (Junsei Chemical, Japan) were added in dehydrated DMF (Aldrich). Stoichiometric amounts of MDI (Kumho Chemical, South Korea) were added to the reaction mixtures while maintaining the reaction temperature at 65–70°C. The total amount of reactants was 200 g for each synthesis. The reaction was continued until it was impossible to stir the reaction mixture having 50 wt% of DMF, and then the methanol was introduced to the mixture to terminate the reaction. The polymerization time was 2–3 h depending on the formulation.

SPU molecular weights were determined using Waters 600 GPC system. Tetrahydrofuran(THF) as a solvent was used with a flow rate of 1.0 ml/min through four Waters Stragel columns of HR1, HR2, HR4 and HR5. The average molecular weights of the samples were calculated in equivalent polystyrene with the calibration curve established from standard samples of polystyrene. Density of SPUs was estimated by the method of additive group contributions [18]. Table 1 summarizes the formulation and characterization of segmented polyurethanes used in this study. The values of hard segment content listed in Table 1 were calculated from the amounts of reactants with the formula of (MDI + EG)/(PTMO + MDI + EG). The hard segment content and its distribution in the polymer chain should depend on the molar ratios of reactants and the reaction condition. The measured values of hard

Table 2
Interaction parameters for solvent-segmented polyurethanes at 20°C

Polymer	χ_{23}(DMF–SPU)	χ_{13}(water–SPU)	
		Measured value	Fit value
SPU-1	0.414	3.42	3.70
SPU-2	0.416	3.14	2.45
SPU-3	0.436	2.57	1.88
SPU-4	0.442	1.95	1.64

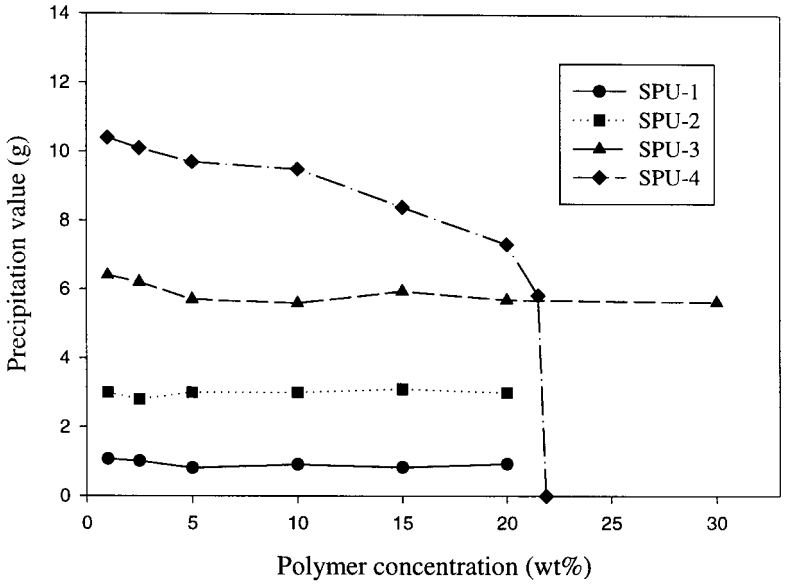

Fig. 1. Precipitation values of water at 20°C as a function of polymer concentration (grams of water per 100 grams of polymer solution in DMF).

segment content may be different from the calculated. Nevertheless, it is considered that the overall results discussed in this manuscript are still valid.

3.2. Cloud point measurement

Cloud point curves were determined by a titration method at 20°C. A flask with a rubber septum stopper was charged with 50 g of polymer solution. Distilled water was introduced into the flask by a syringe through the septum, while thorough mixing was applied using a mechanical stirrer. Composition at the cloud point was determined by measuring the amount of water added when visual turbidity was observed.

3.3. Evaluation of interaction parameters

The nonsolvent-polymer interaction parameter χ_{13} was evaluated by the water sorption method with the Flory–Rehner equation [19]

$$\ln(1-\phi_3)+\phi_3+\chi_{13}\phi_3^2+\frac{V_1\rho}{\overline{M}_c}\left(\phi_3^{1/3}-\frac{1}{2}\phi_3\right)=0 \qquad (3)$$

where ϕ_3 is the volume fraction of polymer, V_1 is the molar volume of nonsolvent, $\overline{M}_c$ is the average molecular weight between two cross-links, and ρ is the density of polymer. This equation was originally derived from the swelling theory for the cross-linked network. Linear polymer can be considered as a swollen gel with cross-links caused by crystalline regions, chain entanglements or Van der Waals interactions. The last term was neglected to obtain the following equation because $\overline{M}_c$ would be quite large for

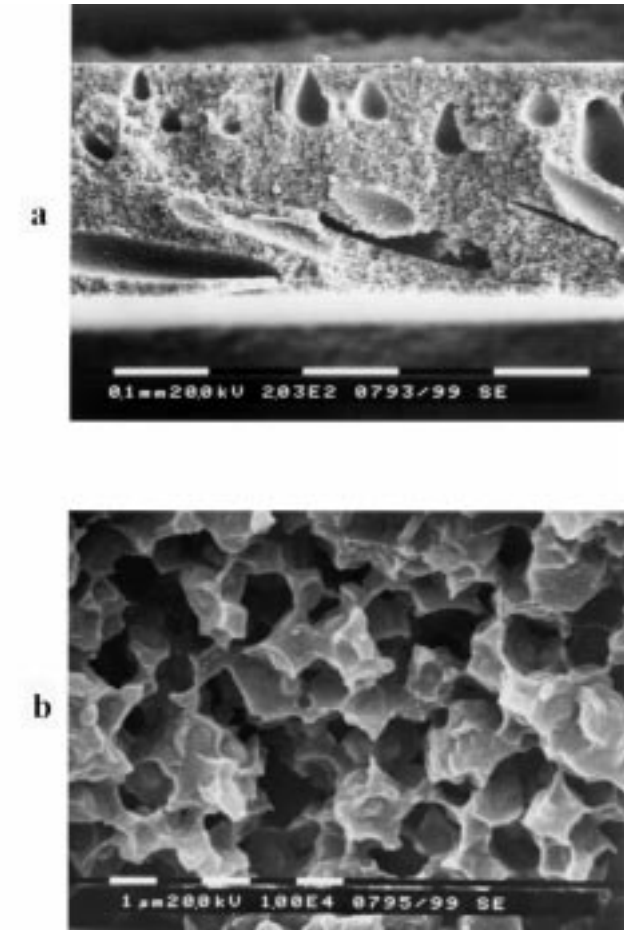

Fig. 2. SEM micrographs of the SPU-4 membrane with 30 wt% dope polymer concentration in DMF and a coagulation bath composition of 50/50 DMF/water: (a) the whole thickness of the membrane and (b) the middle part of the membrane.

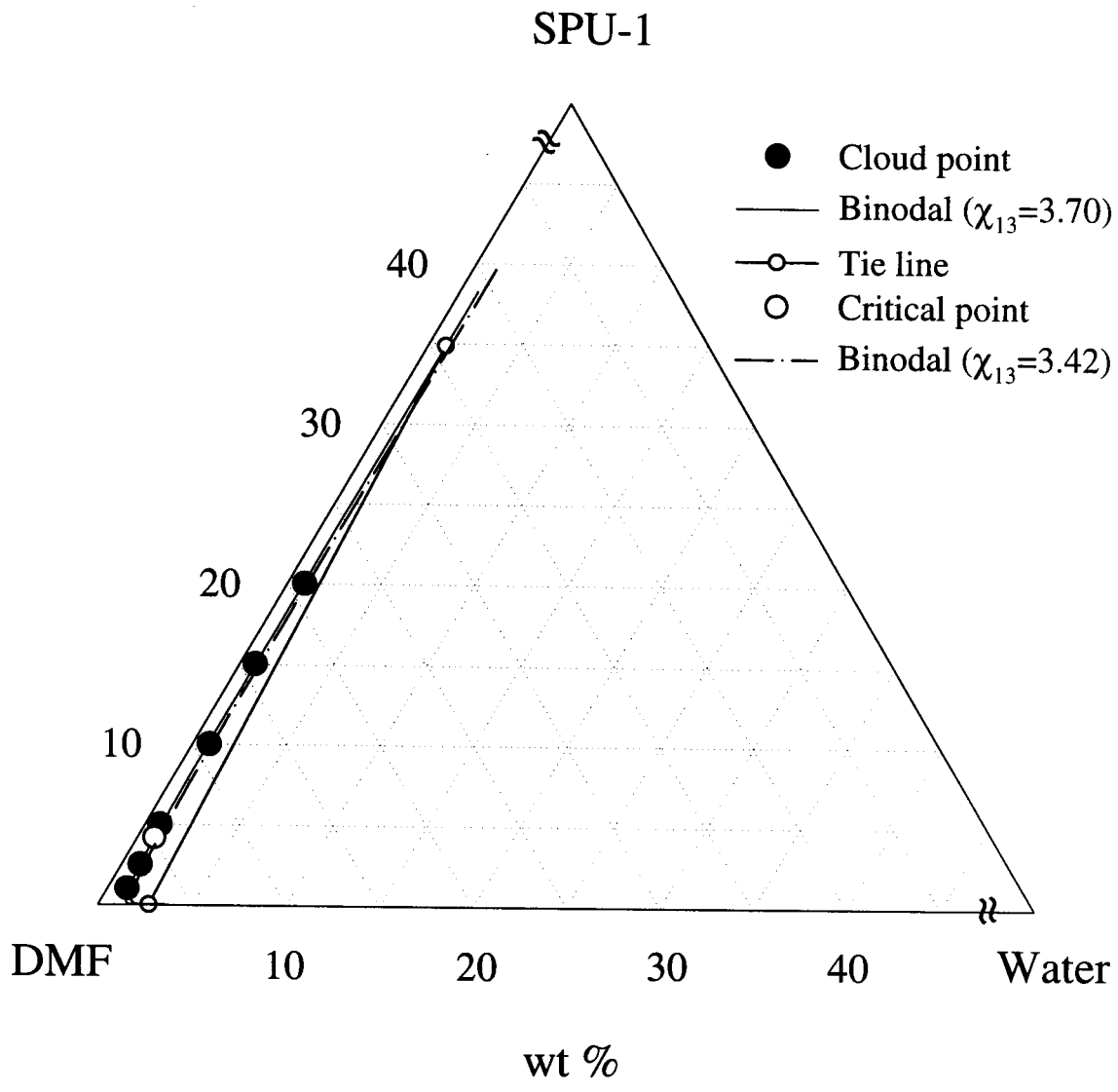

Fig. 3. Cloud point curve at 20°C and calculated phase diagram of SPU-1/DMF/water system.

linear polymer [20]

$$\chi_{13} = \frac{-[\ln(1-\phi_3)+\phi_3]}{\phi_3^2} \quad (4)$$

Dried stripes of homogeneous SPU films (about 0.3–0.4 g with a thickness of 50–70 μm) were immersed in distilled water at 20°C. After 24 h the strips were removed, pressed between tissue papers and weighed. This procedure was continued until no further weight increase was observed and ϕ_3 was calculated from the ratio of dried and water-swollen film.

The solvent-polymer interaction parameter χ_{23} was estimated by the intrinsic viscosity measurement. Solution viscosities of SPU in DMF at 20°C were measured with a Ubbelohde viscometer. The intrinsic viscosity was determined by extrapolating to zero concentration, and the solvent-polymer interaction parameter was obtained by Kok's method [21].

The evaluated interaction parameters of χ_{13} and χ_{23} for the series of polyurethanes are shown in Table 2. The value of χ_{13} for water–SPU-1 (18.6 wt % of hard segment) may not be reliable since the uniform thickness film sample could not be prepared properly (SPU-1 was sticky). The concentration-dependent interaction parameter g_{12} for the water–DMF pair is available from the literature [22].

4. Results and discussion

The DMF–SPU interaction parameter χ_{23}, determined by the intrinsic viscosity measurement, increases slightly with the hard segment content of SPU in the range from 0.414 to 0.442 at 20°C, as shown in Table 2. The χ_{23} (DMF–SPU)

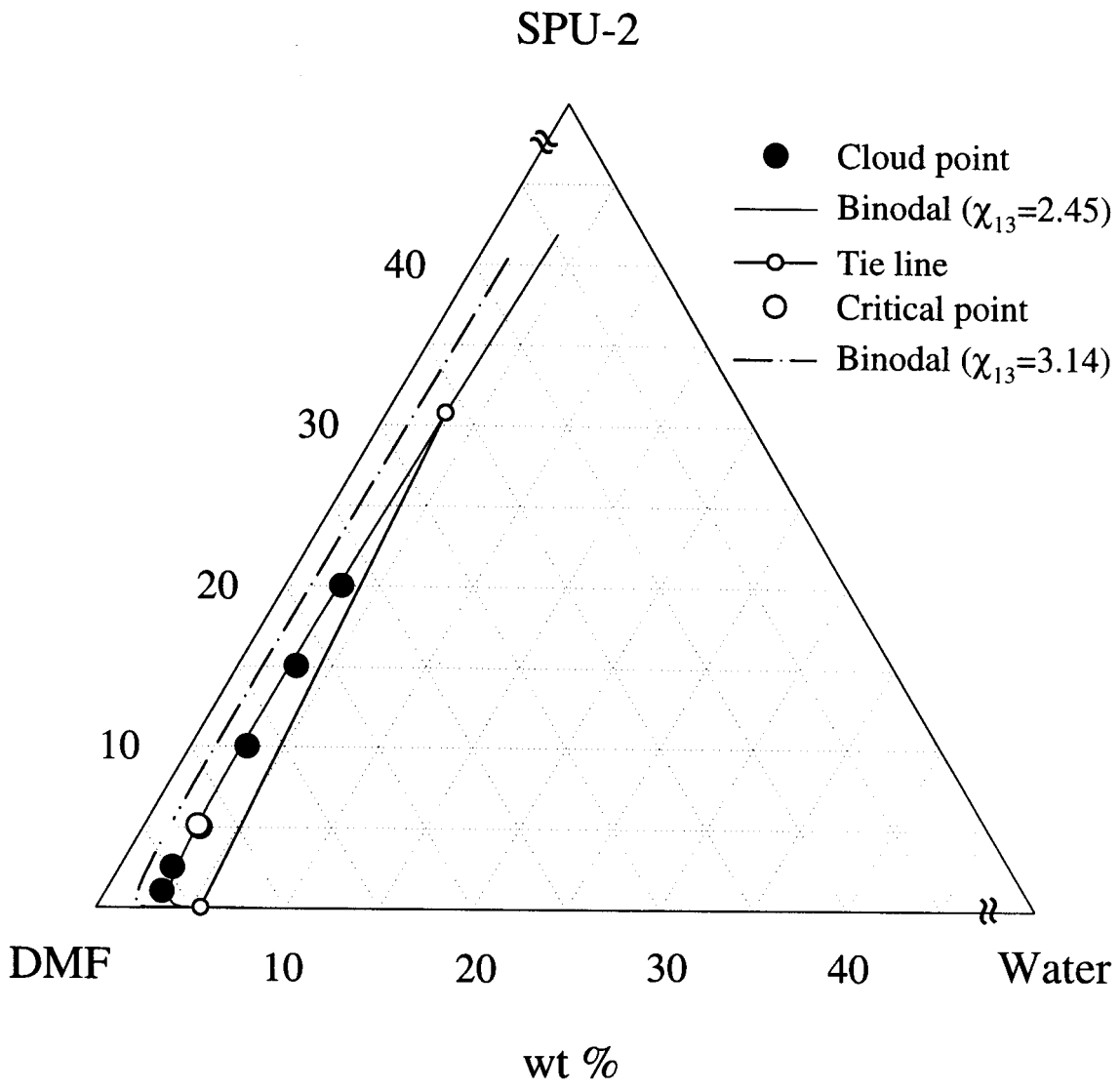

Fig. 4. Cloud point curve at 20°C and calculated phase diagram of SPU-2/DMF/water system.

values in this study are quite high compared to those of DMF and segmented polyester polyurethanes at the same temperature, in which either poly(ethylene adipate)diol or poly(hexamethylene adipate)diol with MDI and EG was used in the synthesis of polyurethanes [23]. These results indicate that the interaction between DMF and the ester group is much stronger than between DMF and the ether group. The values of water–SPU interaction parameter χ_{13}, which were determined by the equilibrium swelling experiment, significantly decreases with increasing the hard segment concentration in the SPU. As will be discussed, the χ_{13} value influences the phase diagram of the SPU/DMF/water system significantly. The decrease of the χ_{13} value with increasing the hard segment concentration is interpreted that the SPU containing higher concentration of the urethane group has more chance to form hydrogen bonding with water. The concentration-dependent interaction parameter g_{12} for the water–DMF system can be found in the literature, and varied from 0.5 to 0.96 with increasing the DMF content [22]. The small value of g_{12} indicates that strong polar interaction exists in the water–DMF mixture.

The results of the titration experiments used to obtain the cloud point curves are shown in Fig. 1, in which the precipitation value of water (grams of water per 100 g of polymer solution in DMF to achieve phase separation) is plotted against the polymer concentration. As the hard segment content in the SPU increased, the amount of water to induce phase separation increased systematically below 20 wt% polymer concentration. The precipitation values for the SPU-4 solution decreased suddenly in a high concentration region and dropped to zero above 21.9 wt%: the 21.9 wt% SPU-4 solution in DMF was hazy at the titration temperature. The titration experiments revealed that the formed precipitate disappeared easily on stirring for the solutions

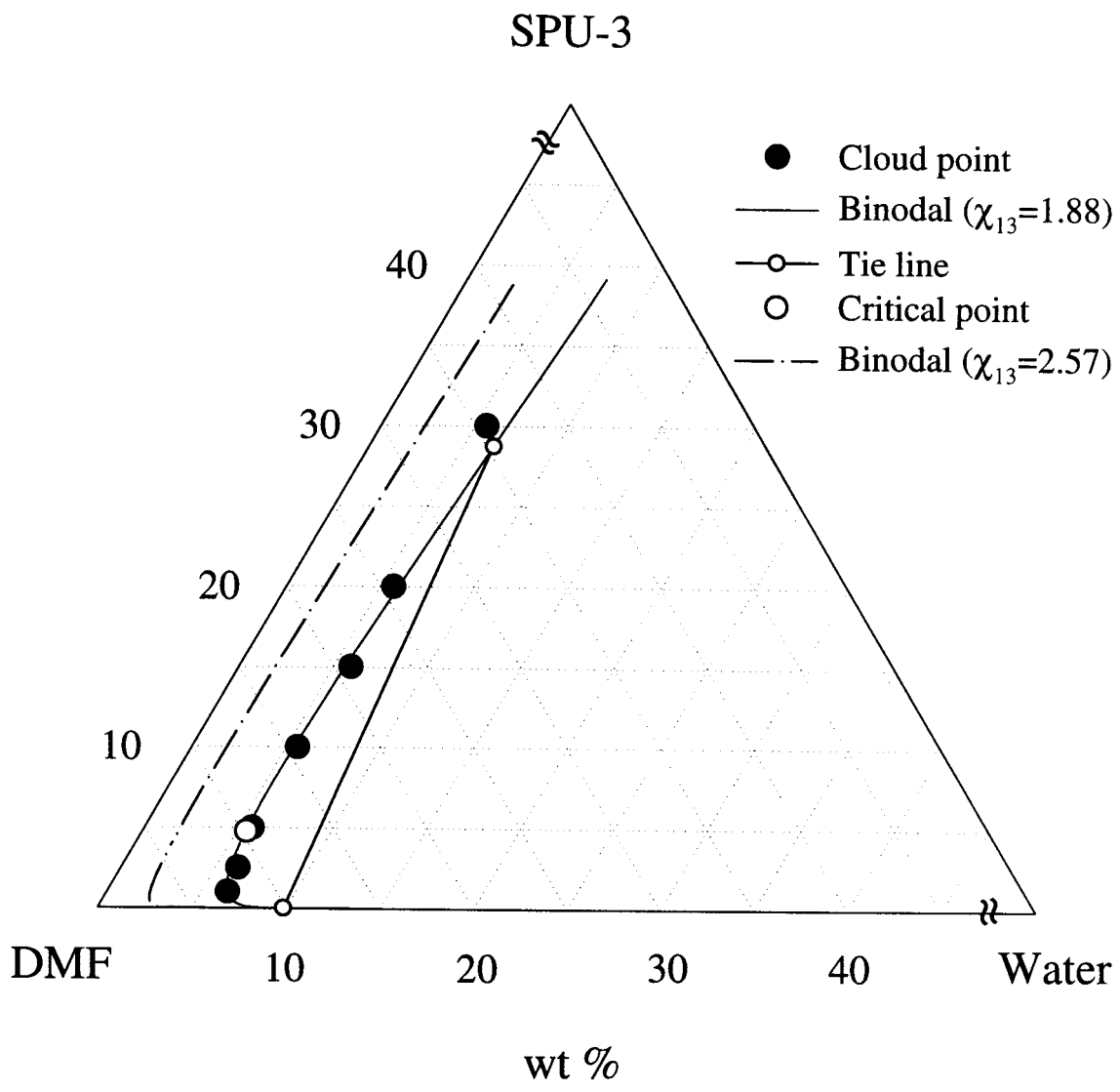

Fig. 5. Cloud point curve at 20°C and calculated phase diagram of SPU-3/DMF/water system.

of SPU-1, SPU-2, and SPU-3 when the amount of water introduced was below the precipitation value. However, the precipitate of SPU-4 solutions near the onset of phase separation was hardly solubilized when the polymer concentration was above 10 wt% and it seemed to result in formation of fine particles on stirring above 20 wt%. We were also able to observe the polyhedron morphology in the cross-section of the SPU-4 membrane prepared by immersion precipitation, which was shown in the magnified micrograph of Fig. 2(b). The polyhedron pore structures are usually observed in membranes of crystallizable polymers [24,25]. Thus liquid–liquid phase separation was coupled with crystallization during membrane formation when the hard segment content in the SPU was high.

One can calculate the phase diagram of a ternary polymer solution in terms of volume fraction of each component given a set of binary interaction parameters and molar volume of each component, based on the Flory–Huggins thermodynamics [22,26]. The parameters needed for calculation of the phase diagram for our system were listed in Tables 1 and 2. Experimental cloud points for the SPU/DMF/water systems were plotted with the calculated phase diagram in Figs. 3–6. The calculated phase diagram includes binodal lines with two different χ_{13} values listed in Table 2, critical compositions and tie lines, and the compositions were converted into weight percentage. The reason why the χ_{13} value was varied on calculating binodal line will be explained later. A small amount of water was needed to induce liquid–liquid phase separation, and the region of the homogeneous phase was enlarged when changing from SPU-1 to SPU-4, which reflects the enhanced hydrophilicity of the polyurethane with increasing polar hard segment content.

The effects of the interaction parameters on the miscibility

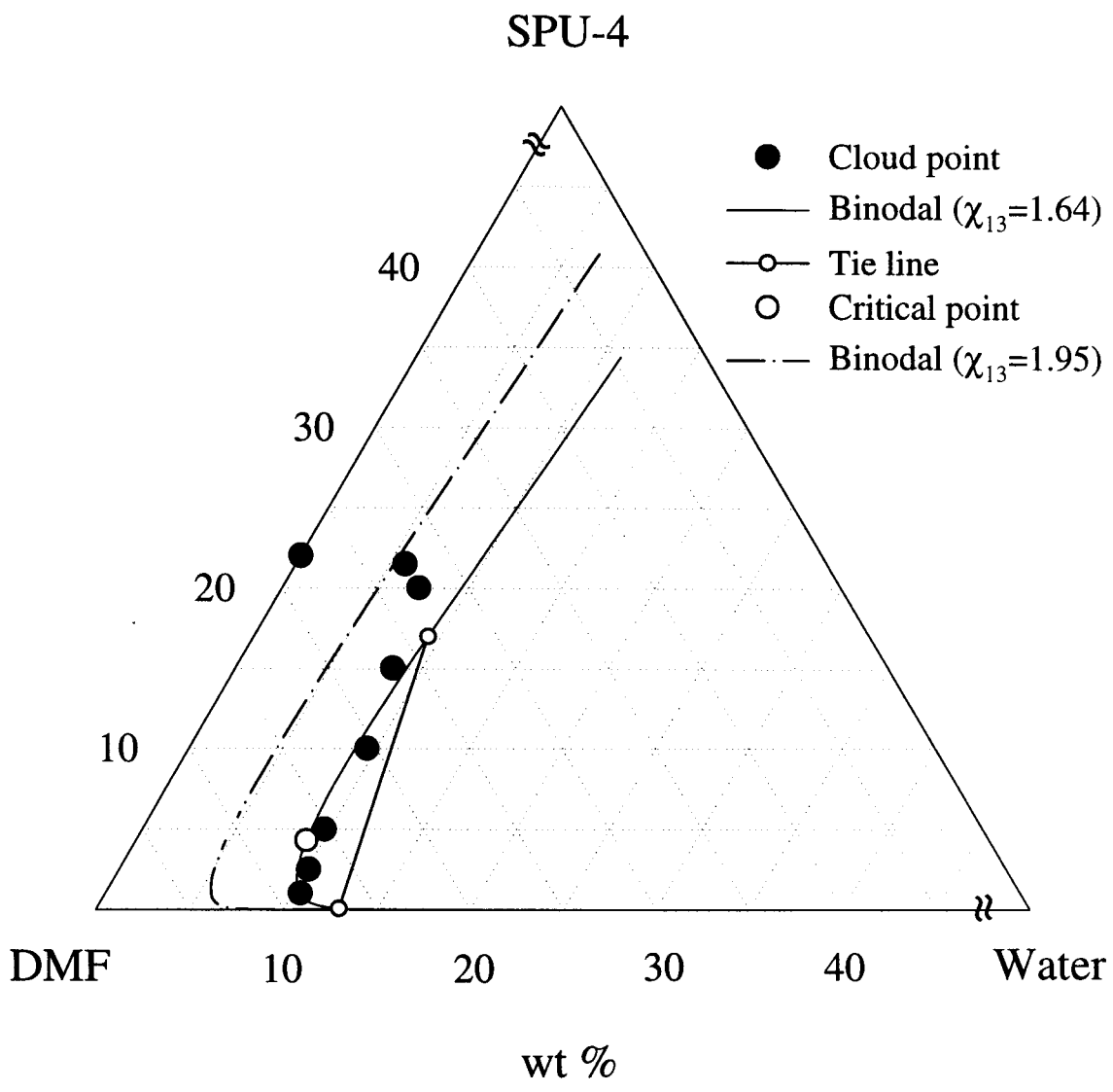

Fig. 6. Cloud point curve at 20°C and calculated phase diagram of SPU-4/DMF/water system.

gap are well described in the literature [17,22,26]. The effect of polymer molecular weight on the phase diagram was reported to be marginal [17]. The location of the binodal line is significantly influenced only when polymer molecular weight is extremely low. When the polymer component is relatively hydrophobic like polysulfone (PSF) and polyethersulfone (PES), the homogeneous region in the phase diagram is enlarged with small χ_{13}, high g_{12}, and small χ_{23}. The χ_{13} effect is most significant and the χ_{23} effect is least. We found similar trend in this study while varying the interaction parameters when calculating the phase diagram. Thus a small amount of water to achieve liquid–liquid phase separation in our system is mainly attributed to the hydrophobicity of SPU and strong interaction between water and DMF. The calculated binodal lines were not in good agreement with the experimental cloud points using the interaction parameters obtained experimentally. Instead we were able to fit the calculated binodal lines with the experimental cloud points, as were shown in Figs. 3–6, by using the measured χ_{23} values and smaller χ_{13} values than those obtained by the equilibrium swelling experiment. The χ_{13} values with which the calculated binodal lines fit the experimental cloud points are indicated in Table 2. Similar trends were also reported for the PES/*N*-methyl-2-pyrrolidone/water system [27] and the PSF/solvent/water system [17]. Because the equilibrium swelling experiment should be carried out in extremely high concentrations of the polymer, the χ_{13} value in the practical concentration range may be lower than that obtained by water sorption technique. In case of SPU-1, the uncertainty in experiment seemed to result in the fit value of χ_{13} larger than the experimental value; films with uniform thickness could not be properly prepared because the SPU-1 was quite flexible and sticky.

Considering the experimental cloud points and the calculated phase diagrams, we observe some interesting features. Liquid–solid phase separation (crystallization) seemed to

be superimposed on the binodal line in the SPU-4 (62.7 wt% of hard segment) system around 20 wt% polymer concentration, which was illustrated in Fig. 6. However, the SPU-3 (47.5 wt% of hard segment) system did not show liquid–solid phase separation up to 30 wt% polymer concentration in Fig. 5. In addition, the slope of the tie line became slightly steeper as the hard segment fraction increased. As the slope of the tie line increases for a given location in the phase diagram, the polymer concentration in the polymer-rich phase may decrease, resulting in the delay of solidification [28]. This feature can significantly influence the final morphology of the membrane in combination with crystallization because the SPUs containing high concentration of hard segment are crystallizable. Depending on the competition between liquid demixing and crystallization, a variety of structures can be formed [29].

The critical compositions are shown as unfilled circles in the calculated binodal lines in Figs. 3–6. The polymer concentrations at critical point were around 5 wt% in all cases. The critical composition determines which phase is nucleated for the nucleation and growth process during membrane formation. There are two possibilities, depending on the composition of initial polymer solution, with respect to the critical point. For $\phi_3 > \phi_{cr,3}$, where $\phi_{cr,3}$ is the polymer concentration at critical point, the nuclei of the polymer-lean phase will form. For $\phi_3 < \phi_{cr,3}$, the nuclei of the polymer-rich phase will form and precipitate. When phase separation starts at the critical composition ($\phi_3 = \phi_{cr,3}$), the structure formation is dominated by the spinodal decomposition [30]. A typical membrane forming solution contains higher than 10 wt% of polymer concentration. In such a case, phase separation occurs by nucleation of the polymer-lean phase, assuming that phase separation occurs by the mechanism of nucleation and growth.

5. Conclusions

The effects of the hard segment content in the segmented polyurethane on liquid–liquid phase separation of the SPU/DMF/water system were studied. The hard segment content in SPU was controlled by changing the molar ratio of MDI and PTMO on the SPU preparation. The cloud points were obtained by a titration method and the phase diagrams were calculated based on the Flory–Huggins lattice treatment. As the hard segment fraction in SPU increased, the DMF–SPU interaction parameter χ_{23} increased slightly and the water–SPU interaction parameter χ_{13} decreased significantly.

The amount of water to achieve liquid–liquid phase separation increased systematically with increasing the hard segment content. When the hard segment content was low, the amount of water to obtain liquid demixing was extremely small. Liquid–liquid phase separation was coupled with crystallization when the SPU had high concentration of the hard segment. These coupled phenomena in combination with the phase segregation in SPU arising from the incompatibility between the hard and soft segments may be utilized to produce a variety of morphologies in polyurethane membranes prepared by immersion precipitation.

Acknowledgements

This study was partially supported by the Chungwoon University.

References

[1] Lamba NMK, Woodhouse KA, Cooper SL. Polyurethanes in biomedical applications. New York: CRC Press, 1998.
[2] Lyman DJ, Fazzio FJ, Voorhees H, Robinson G, Albo D. J Biomed Mater Res 1978;12:337.
[3] Chian KS. J Appl Polym Sci 1997;65:1947.
[4] Gaides GE, McHugh AJ. Polymer 1989;30:2118.
[5] Aubert JH. Macromolecules 1988;21:3468.
[6] Vadalia HC, Lee HK, Myerson AS, Levon K. J Membr Sci 1994;89:37.
[7] Mulder MHV. Basic principles of membrane technology. Amsterdam: Elsevier, 1991.
[8] Li Y, Kang W, Stoffer JO, Chu B. Macromolecules 1994;27:612.
[9] Chu B, Gao T, Li Y, Wang J, Desper RC, Byrne CA. Macromolecules 1992;25:5724.
[10] Chang SL, Yu TL, Huang CC, Chen WC, Linliu K, Lin TL. Polymer 1998;39:3479.
[11] Miller JA, Lin SB, Hwang KKS, Wu KS, Gibson PE, Cooper SL. Macromolecules 1985;18:32.
[12] Martin DJ, Meijs GF, Gunatillake PA, Yozghatlian SP, Renwick GM. J Appl Polym Sci 1999;71:937.
[13] Wienk IM, Boom RM, Beerlage MAM, Bulte AMW, Smolders CA, Strathmann H. J Membr Sci 1996;113:361.
[14] VandeWitte P, Dijkstra PJ, VandenBerg JWA, Feijen J. J Polym Sci, Polym Phys Ed 1997;35:763.
[15] Flory PJ. Principles of polymer chemistry. Ithaca, NY: Cornell University Press, 1953.
[16] Tompa H. Polymer solutions. London: Butterworths, 1956.
[17] Kim JY, Lee HK, Baik KJ, Kim SC. J Appl Polym Sci 1997;65:2643.
[18] Van Krevelen DW. Properties of polymers: their correlation with chemical structure; their numerical estimation and prediction from additive group contributions. 3rd ed. Amsterdam: Elsevier, 1990 (p. 71 and 129).
[19] Flory PJ, Rehner J. J Chem Phys 1943;11:521.
[20] Mulder MHV, Smolders CA. J Membr Sci 1984;17:289.
[21] Kok CM, Rudin A. J Appl Polym Sci 1982;27:353.
[22] Altena FW, Smolders CA. Macromolecules 1982;15:1491.
[23] Kim YD, Kim JY, Lee HK, Kim SC. J Appl Polym Sci 1999;73:2377.
[24] Bulte AMW, Folker B, Mulder MHV, Smolders CA. J Appl Polym Sci 1993;50:13.
[25] Cheng LP, Dwan AH, Gryte CC. J Polym Sci, Polym Phys Ed 1995;33:211.
[26] Yilmaz L, McHugh AJ. J Appl Polym Sci 1986;31:997.
[27] Zeman L, Tkacik G. J Membr Sci 1988;36:119.
[28] Kim JY, Kim YD, Kanamori T, Lee HK, Baik KJ, Kim SC. J Appl Polym Sci 1999;71:431.
[29] Lee HK, Levon K. Polymer (Korea) 1997;21:241.
[30] Broens L, Altena FW, Smolders CA. Desalination 1980;32:33.